Evaluation of Heat Loss to Cylinder Wall of Compression Ignition Engine by Heat Transfer Models

Shahzad Bobi[1] and Yossapong Laoonual[2,*]

ARTICLE INFO

Article history:
Received: 17 February 2021
Revised: 2 June 2021
Accepted: 16 June 2021

Keywords:
Fuel injection pressure
Engine speed
Heat release rate
Heat transfer coefficient
Compression ignition engine

ABSTRACT

Modelling of cylinder heat transfer and wall heat loss are critical tasks for evaluating the energy flow in the engine. This work provides knowledge in this field under high fuel injection pressure and variable engine speed. First, the experimental approach was used to acquire some primary parameters, including the cylinder volume and pressure at every 0.1 crank angle degree. The engine was set to run at 1400 rpm to 2400 rpm with 200 incremental at full load and fuel injection pressure varied at 40 MPa, 90 MPa, and 110 MPa. The obtained secondary parameters included cylinder temperature to evaluate convective heat transfer coefficient (CHTC), heat flux, and cylinder gas velocity. Two models were employed for the assessment of the CHTC through Woschni and Hohenberg models. The outcomes of the experimental work revealed that the CHTC and heat flux versus crank angle degree were accomplished from both models with low, medium, and high injection pressure at each engine speed. However, the results indicate that the CHTC from the Woschni model is higher than the Hohenberg correlation model. The peaks value of the CHTC from the Woschni model at higher fuel injection pressure increases by 21.7%, 27.1%, and 16.4% at low, medium and high speeds, respectively.

1. INTRODUCTION

The heat loss contributes to a substantial impact on fuel consumption, engine performance improvement, and engine-out emission reduction [1], [2], [3], [4], [5]. Therefore, it is significant to comprehend heat transfer in an internal combustion engine (ICE), which plays a critical role in modern engine development, such as the thermodynamic processes, the engine parts' toughness, and design associated with weight.

Many research have been carried out throughout the last few decades to examine the combustion analysis, heat transfer, heat release rate, and heat flux in the ICE [6], [7], [8]. Fig. 1 shows examples of areas of interest in the combustion analysis in ICE. Arato and Takashima [9] investigated the influence of combustion chamber geometry on heat loss in order to optimize fuel economy by changing the compression ratio. Their results showed that the fuel injection area causes high cylinder temperature, which was the reason for higher heat loss to the combustion chamber wall. In a homogeneous charge compression ignition engine, Hairuddin et al. [10] investigated the impact of different heat transfer models (Woschni, modified Woschni, and Hohenberg models) in homogenous charge compression ignition (HCCI) engine. The modified Woschni model was found to be the best option due to its high rate of heat release and low rate of heat loss. The modified Woschni model was found to be the best option because of its high rate of heat release and low rate of heat loss. However, they asserted that the fundamental constants of the Woschni and Hohenberg model could be used in the HCCI engine. Irimescu [11] developed the heat transfer coefficient for turbulence stream in tubes to ICE in motoring condition and compared with computation fluid dynamics (CFD) measurements, compared with Annand and Woschni models. The finding of this work revealed that the heat transfer rate was in limitation with each model, and modification in the Equation was not essential. Trujillo et al. [1] employed a single-cylinder air-cooled engine with various loads to estimate the cylinder temperature via simulation and experimental approaches. Heat flux and instantaneous CHTC were calculated using the estimated cylinder temperature as a suitable parameter to assess heat loss from cylinder gases to combustion chamber walls.

A nonlinear relationship was found between cylinder temperature and engine speed, with higher engine speed resulting in lower mean cylinder gas-side surface temperatures. Furthermore, the instantaneous CHTC grew

[1]*The Joint Graduate School of Energy and Environment, (JGSEE), 126 Pracha Uthit Road, Bang Mod, Thung Kru, Bangkok 10140, Thailand.*
[2]*Department of Mechanical Engineering, King Mongkut University of Technology, (KMUTT), 126 Pracha Uthit Road, Bang Mod, Thung Kru, Bangkok 10140, Thailand.*
**Corresponding author:* Yossapong Laoonual; Phone: +66-89-138-1484; Email: yossapong.lao@kmutt.ac.th.

almost linearly with engine speed under all engine loads. Menacer et al. [12] reported that various models are used to determine the CHTC and found that the peak values are not of the same level even with the identical engine and experimental conditions. The major reason was that the models were based on turbulent heat transfer in a tube. Overall, different models have been employed in earlier studies to estimate heat transfer at various engine speeds and loads in a CI engine. However, the impact of common-rail pressure on CHTC is not deeply explored.

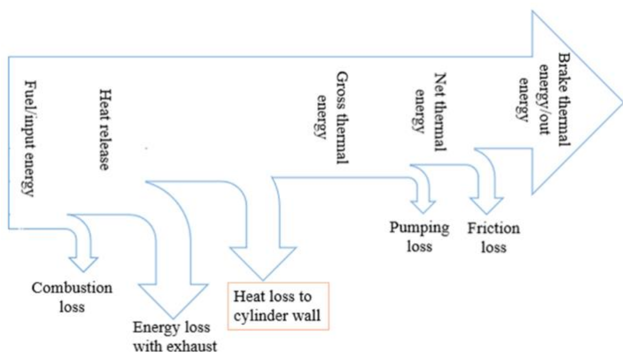

Fig. 1 Energy flow in an internal combustion engine.

Herein, the heat loss to the combustion chamber wall is estimated by two commonly used heat transfer models, Woschni and Hohenberg models. This work aims to explore the consequence of the fuel injection pressure such as 40 MPa, 90 MPa, and 110 MPa with low, medium, and high engine speeds at full load to evaluate the heat exchange from combustion gases to the combustion chamber wall. For this purpose, the widely used models, Woschni and Hohenberg, have been employed to estimate the CHTC in a CI engine using diesel fuel. We use these parameters in Woschni and Hohenberg models to analyze heat loss. The main investigated parameters are cylinder pressure and temperature employed to estimate the CHTC and cylinder gas velocity.

2. METHODOLOGY

2.1 Experimental setup and procedure

This study was based on experiments and numerical simulations. In the experiment, the working fluid in a CI engine is considered a thermodynamic system that suffers mass/energy exchange with the environment. Because of this, the heat release rate in combustion is determined by the first law of thermodynamics. Herein, experimental pressure data are applied in the thermodynamic models to compute heat release rate, cylinder temperature, instantaneous CHTC, and heat flux for the analysis.

The engine setup of this experiment is demonstrated in Fig. 2. In Fig. 2a, a modified compression ignition (CI) engine with the water-cooling system is shown, and Fig. 2b describes the schematic diagram of the experimental setup. The engine used in this work had a displacement of 709cc and was a 4-stroke single-cylinder CI (bore 97mm and stroke 96mm). Table 1 provides engine specifications. The compression ratio of engine 18 was connected to a water cold eddy current dynamometer (NEDD130H) to adjust engine torque in the range of 25kg.m. A laminar airflow meter (Sokken LFE25B with a digital manometer) measures differential intake air pressure in kPa with accuracy: ± 0.3%. A high-pressure direct injection system with a six-hole electronic fuel injector, each having 0.14 mm diameter, was employed to inject fuel at high pressure. A close system was developed for accurate measurements of fuel flow rate, whereas the fuel added from the return lines of injector, common-rail, and the high-pressure fuel pump was connected after the low-pressure fuel pump to the main fuel supply. The instantaneous cylinder pressure data were collected using a pressure transducer (Kistler 6052C), having a pressure range from 0 to 250 bar and a sensitivity of 20.2 pC/bar mounted at a cylinder head. Additionally, a combustion analyzer model (Kistler Kibox 2893) was used to evaluate the combustion characteristics. The incremental rotary encoder was employed to determine the crankshaft position.

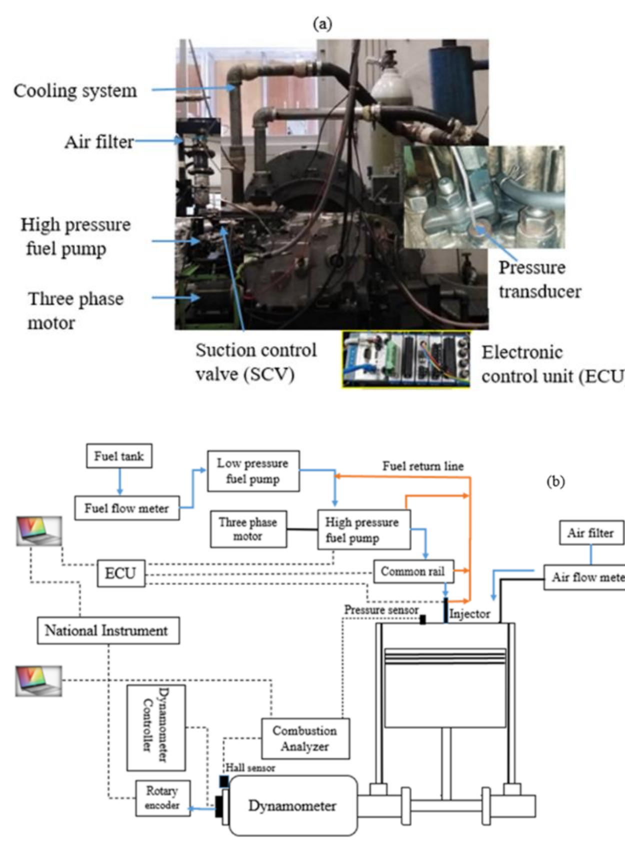

Fig. 2 Experimental setup (a) actual and (b) schematic diagram of a single-cylinder compression ignition engine.

Table 1. Specification of compression ignition engine

Engine	Kubota 140
Displacement (cm^3)	709
Bore × stroke (mm)	97 × 96
Compression ratio (CR)	18
Number of an injector nozzle hole	6
Diameter injector nozzle hole (mm)	0.14
Max. net torque at 1600 RPM (kg.m)	5.0
IVO (bTDC)	5
IVC (aTDC)	35
EVO (bBDC)	5
EVC (aBDC)	15
Cooling system	Water

Fuel properties mainly, cetane number, have an essential effect on combustion characteristics. The test fuel (Euro-5 diesel) used in this experiment was acquired from the Bangchak Corporation Public Limited Thailand. The fuel was tested under the American Society for Testing and Materials (ASTM) standards. The chemical properties of test fuel are described in Table 2.

Table 2. Chemical properties of the testing fuel

Density at 15 ºC (g/cm^3)	ASTM D4052-16	0.815
Kinetic viscosity at (40 ºC) @ cSt	ASTM D445-17a	3.445
Flashpoint (ºC)	ASTM D93-16a	78
Cetane number	ASTM D976	64
Water content (mg/kg)	ASTM E1064	96
Sulfur content (ppm, wt)	ASTM D2622-10	1.1

2.2 Test conditions

The test conditions of this experimental work are illustrated in Table 3. The fuel injection timing was adjusted at 15bTDC, which differentiate it from a conventional CI engine. In order to vary the injection pressure to 40 MPa, 90 MPa, and 110 MPa while under full load, a common-rail with high-pressure fuel injection system was used. The injection pressure and modern emissions regulated Euro-5 diesel fuel was applied for the analysis at the engine speeds of 1400 rpm, 1600 rpm, 1800 rpm, 2000 rpm, 2200 rpm, and 2400rpm. We categorized the engine speeds into three groups: low (1400 to 1600 rpm), medium (1800 to 2000 rpm), and high (2000 to 2400 rpm), to understand the consequences of fuel injection pressure. A National Instrument LABVIEW program-controlled an electronic control unit (ECU) to regulate the injection timing, fuel injection duration, and injection pressure. The heat release rate was measured through cylinder pressure data collected throughout 100 cycles on average. All data were sampled at a sampling rate of 0.1 CA.

Table 3. Experimental conditions

Injection timing (bTDC)	Fuel injection pressure (MPa)	Engine speed (RPM)		Engine torque (Nm)
-15	40	1400	Low	48.02
		1600		49.00
	90	1800	Medium	48.02
		2000		46.06
	110	2200	High	44.10
		2400		40.95

2.3 Heat release rate (HRR)

Statistics about combustion processes, such as ignition delay, low-temperature reaction, premixed combustion, and mixing controlled combustion, including the late combustion phase, can be derived from the computation of heat release rate. The rate of heat release was calculated based on energy conservation law or the first law of thermodynamics as demonstrated in differential form in Equations (1) and (2) [13], [14], [15]. The heat release rate is the function of calorific value, combustion velocity of the fuel, and combustion temperature. Woschni and Hohenberg models were used to calculate the heat loss from the combustion chamber wall. An example of energy balance in a CI engine fueled by Euro-5 diesel is illustrated in Fig. 3.

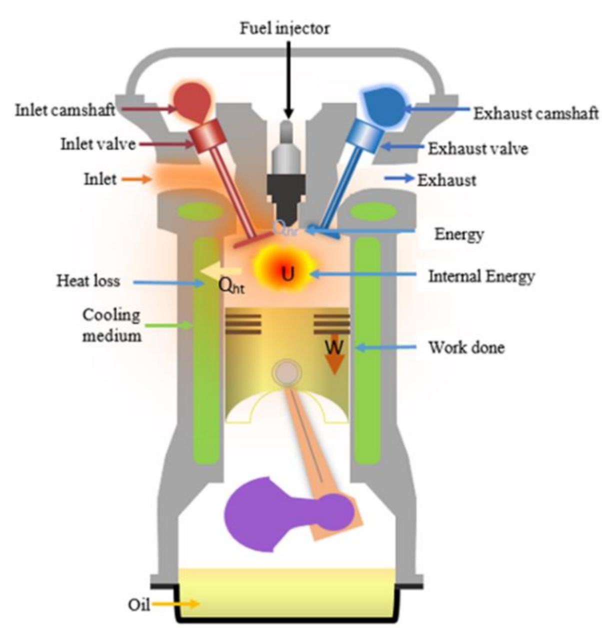

Fig. 3 Energy balance of the engine.

$$dQ_{hr} = dU + dW + dQ_{ht} \quad (1)$$

$$\frac{dQ_{hr}}{dt} = \frac{dU}{dt} + \frac{dW}{dt} + \frac{dQ_{ht}}{dt} \quad (2)$$

where dQ_{hr}/dt represent the heat release rate in the system, dU/dt represent the rate of change in internal energy, and dW/dt represent the rate of work done by the system, dQ_{ht}/dt represent the rate of heat loss to the cylinder wall from the system. The explanation of Equations (1) and (2) have been given in section 2.4. Since work done and internal energy definition are implemented, and differentiating in ideal gas law ($PV = mRT$) leads to result like this; $dW/dt = PdV/dt$ and $dU/dt = mC_v dT/dt$.

Equation (3) can be employed to calculate the heat release rate as a function of CA after time has been substituted (t).

$$\frac{dQ_{hr}}{d\theta} = \frac{\gamma}{\gamma-1}\left(P\frac{dV}{d\theta}\right) + \frac{1}{\gamma-1}\left(V\frac{dP}{d\theta}\right) + \frac{dQ_{ht}}{d\theta} \quad (3)$$

where $dQ_{hr}/d\theta$ is the heat release rate due to combustion per CA (J/CA), γ represents the specific heat ratio of C_p/C_v, and P, V and θ are the instantaneous cylinder pressure, volume and CA.

2.4 Heat transfer models

Heat transfer from the combustion gases to cylinder walls is through convection and radiation during the combustion process. Inhomogeneous charge in CI engines, the radiation effect is not considered to investigate the combustion process or heat transfer calculations. For this, the CHTC rate can be expressed based on Newton's law of cooling, as demonstrated by Equation (4) [2], [11], [16], [18].

$$Q_{ht} = h_c A_c (T_g - T_w) \quad (4)$$

where Q_{ht} represents the heat transfer from the combustion gases to the cylinder wall (kW); h_c represents the convective heat transfer coefficient of the gas (W/m^2. K); A_c represent the combustion chamber area (m^2); ($T_g - T_w$) signifies the temperature change amongst cylinder gas and combustion chamber wall (K), and T_w represent the mean wall temperature (K). In the works of Stone [19] and Falcone et al. [20], the T_w of 350K and 650K, respectively, were employed as the mean wall temperatures. However, the T_w depends on combustion and coolant temperature, combustion chamber wall materials, inlet temperature, equivalence ratio, engine speed, and load. On the other side, Wang and Berry [7] employed the wall temperature of around 393K, whereas Zak et al. [2] used the wall temperatures of 410K and 480K in zones I and II at 1800 rpm. Rakopoulos et al. [15] examined the negligible effect of wall temperature as varied from 400K to 900K with an increment of 100K on cylinder pressure and engine output power during combustion. For this study, the mean wall temperature of 450K is selected among the value used by many researchers and assumed constant throughout the test.

In the case of models, different models were used to calculate the CHTC in spark ignition (SI) and CI engines. In this work, Woschni and Hohenberg models were applied to estimate the CHTC Equation (5) was applied to compute the heat loss from combustion gases to the cylinder wall [10], [21]. Combustion gas temperature $T_g = T$ was used to estimate CHTC and was calculated through ideal gas law.

$$\square_c = 3.26B^{-0.2}P^{0.8}w^{0.8}T^{-0.55} \quad (5)$$

where P_g and V_g represents the cylinder gas pressure and volume, respectively. The Equation (6) expresses the cylinder gas velocity.

$$w = C_1 S_p + C_2 \frac{V_d T_{IC}}{P_{IC} V_{IC}} (P_{firing} - P_{motoring}) \quad (6)$$

As shown in Equation (6), C_1 and C_2 are the fixed parameters. Woschni recommended the following value for the specified parameters. Combustion and expansion stroke: C_1 = 2.28 and C_2 = 0.00324; intake and exhaust stroke: C_1 = 6.18 and C_2 = 0; compression: C_1 = 2.28, C_2 = 0. S_p represents the mean piston speed computed through $2LN$ (m/s), N is the engine speed (rpm), and L is the stroke length (m). V_{IC}, P_{IC}, T_{IC} are the volume (m^3), pressure (kPa), and temperature (K) of the gas in-cylinder as intake valve is closed; P_{firing}, $P_{motoring}$ are cylinder pressure during combustion and motoring mode (kPa), respectively [10], [21], [22], where w represents the velocity of local cylinder gas (m/s).

The instantaneous wall area of the combustion chamber Ac (m^2) is given as a summation of the cylinder head, cylinder wall area, and piston head. The A_c was expressed in Equation (7) and computed per CA [21].

$$A_c = \pi\frac{B^2}{4} + \left[\pi\frac{B^2}{4} + \frac{4Vc}{B}\right] + \pi\frac{L^2}{4}\left[\left(R + 1 - cos(\theta) - \sqrt{(R^2 - sin^2(\theta))}\right)\right] \quad (7)$$

where B represents the cylinder bore (m), V_c is clearance volume (m^3), $R=2l/L$ (L is the stroke length, l represents the length of connecting rod (m)). Interestingly, Hohenberg found that the Woschni model has over-predicted the mean heat flux thru the engine cycle due to underestimating the CHTC during the compression stroke. The overestimation affects the CHTC throughout the combustion process. Thus, Hohenberg expressed the improved model with the implementation of cylinder volume rather than cylinder bore and the addition of mean piston speed as described in Equation (8) [10], [21], [23].

$$h_c(\theta) = 3.26P(\theta)^{0.8}T(\theta)^{-0.4}V(\theta)^{-0.06}(\overline{S}_p + c)^{0.8} \quad (8)$$

where P, V, T denotes the cylinder pressure (kPa), volume (m^3), and temperature (K) applied per CA; S_p represents the mean piston speed (m/s), and c is denoted as calibration factor equals to 1.4 as suggested Hohenberg.

Thus, heat flux was computed through Woschni and Hohenberg heat transfer coefficient Equation (9) [24].

$$Q_f = h_c(T_g - T_w) \quad (9)$$

where, Q_f is the heat flux in (kW/m^2) to be estimated by Woschni and Hohenberg models.

3. 3. RESULTS AND DISCUSSION

3.1 Cylinder pressure and temperature

Figure 4 depicts the effects of fuel injection pressure and engine speed on cylinder pressure per CA under full load. The pressure data as measured through a pressure sensor are presented as an average of 100 cycles. As shown in Fig. 4, all curves exhibit a similar upward and downward trend in-cylinder pressure in compression and expansion strokes.

Although the injection timing was 15 bTDC which is not similar to a traditional CI engine, the peaks of cylinder pressure occurred slightly after the top dead center. The highest peaks were 88, 85, 83, and 73 bar investigated at 2200, 2000, 1800 and 1400 rpm. At these high pressures and diesel properties, the air-fuel mixture is expected to have enough time for proper mixing, and combustion can occur before top dead center. Contrary, the trend of cylinder pressure at high-speed of 2400 rpm and injection pressure of 110 MPa was observed to be similar to that of low speeds (1400 rpm and 1600 rpm at 40MPa for low speed). The reason for this is that at high speed and high injection pressure, the fuel penetrates at the piston head and combustion chamber wall, indicating insufficient time to vaporize the fuel and air mix. As a result, incomplete combustion, low heat release rate, and low cylinder pressure occur. In the case of low injection pressure and low engine speed, fuel does not vaporize appropriately due to low cylinder air temperature, resulting in a low heat release rate.

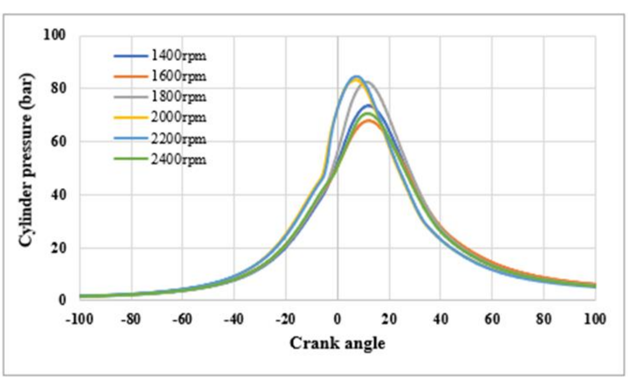

Fig. 4. Cylinder pressure versus crank angle at low, medium, and high engine speeds.

In Fig. 5, the cylinder temperature curves of 2000 rpm at 90 MPa and 2200 rpm at 110 MPa are seen not to follow the cylinder pressure. This could be because of premixed combustion, which results in low cylinder temperatures and increased heat loss to the cylinder wall. However, the cylinder temperature increased dramatically after ignition until it reached its maximum and then decreased slightly. The peak of cylinder temperature for 1800 rpm with an injection pressure of 90 MPa followed the cylinder pressure of other speeds.

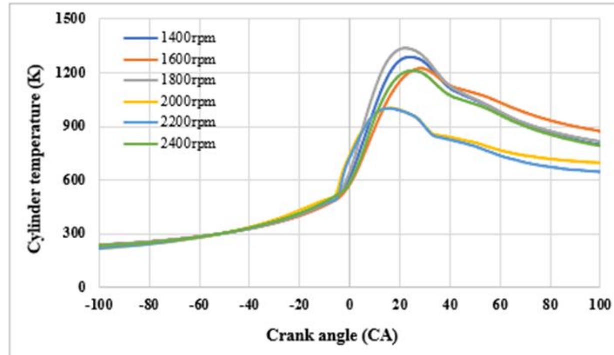

Fig. 5. Cylinder temperature versus crank angle at low, medium, and high engine speeds.

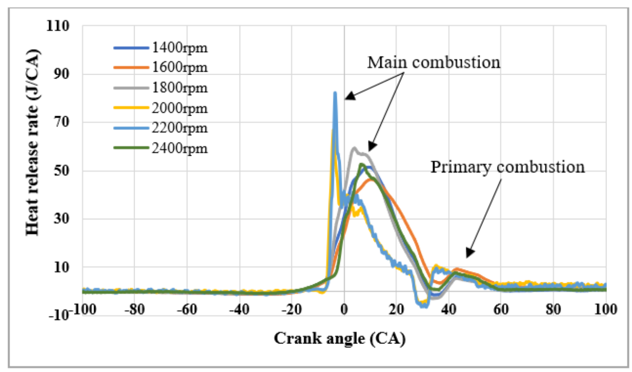

Fig. 6 Heat release rate versus crank angle at low, medium, and high engine speeds.

3.2 Heat release rate (HRR)

Equation (3) defines the heat release rate, which is denoted by $dQ_{hr}/d\theta$. Figure 6 depicts the heat release rate data as a function of CA for fuel injection pressure (40 MPa, 90 MPa, 110 MPa), engine speeds (low, medium, and high), and full load. It can be seen that those two peaks of rate of heat release emerge. The first peak is due to the main combustion process, while the second peak is due to the secondary combustion in the mixing control phase. The main combustion occurs earlier and attains a higher peak because of the fast combustion process, whereas the secondary combustion occurs later with a low peak due to unburned lean homogeneous mixture and locally lean/rich stoichiometric mixture [25], [26]. In terms of combustion duration, the mixing controlled combustion phase reveals a more extended combustion period. As observed in Fig. 6, in all engine speeds and injection pressures, the heat release rate sharply increased in the premixing phase and rose until its peak after the top dead center (termed as diffusion combustion phase and mixing control phase). However, the lowest peaks of heat release rate were investigated in the highest engine speed (2400 rpm at

110MPa) and lowest engine speeds (1400 and 1600 rpm at 40 MPa).

This is mainly caused due to poor air-fuel mixing. Conversely, the highest peaks of heat release rate were achieved at 2000 rpm (90 MPa) and 2200 rpm (110 MPa) because of proper vaporization of fuel and air-fuel mixing [27]. The highest heat release peaks indicate that more fuel was consumed during the premixed combustion phase [28].

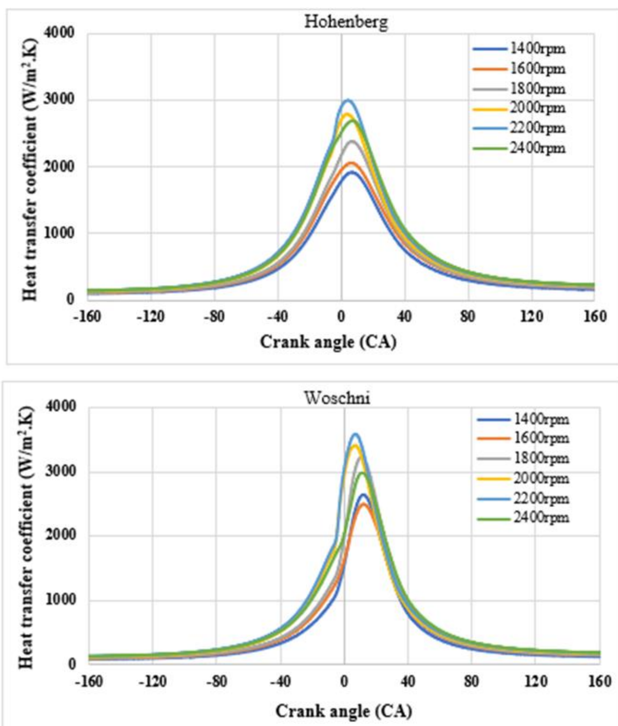

Fig. 7. Heat transfer coefficient versus crank angle at low, medium, and high engine speeds for Woschni and Hohenberg models.

3.3 Convective heat transfer coefficient (CHTC)

The instantaneous CHTC, represented by h_c, from Woschni and Hohenberg models is shown in Fig. 7. Equations (5) and (8) are used to compute these models as described in section 2.4. However, the parameters applied on both models were fuel injection pressure (40 MPa, 90 MPa, and 110 MPa) and engine speeds (low, medium and high) to evaluate the heat loss from the cylinder gases to the cylinder wall. The results showed a similar increasing trend of CHTC per CA in compression stroke until its peaks after top dead center in all engine speeds. From Fig. 7, trends of peak values of CHTC for Woschni and Hohenberg models follow the trends as cylinder pressure. It was noted that, in the Woschni model, at 1400 rpm (40 MPa), 1800 rpm (90 MPa), and 2200 rpm (110 MPa), the peak value of the CHTC were approximately 2484 W/m^2. K, 3210 W/m^2.K, and 3580 W/m^2.K, respectively, after top dead center. However, these results were higher than those of the Hohenberg model by 21.7%, 27.1% and 16.4%, respectively. The study of Sanli et al. [29] employed Woschni and Hohenberg models at 30 Nm (full load) and 2000 rpm and revealed similar increasing trends but higher peaks values of CHTC in the Woschni model than Hohenberg and Han models. Similarly, Hairuddin et al. [10] reported a higher peak value of CHTC from the modified Woschni model when operated the engine at 900 rpm and 40℃ intake air temperature. They suggested that the change in peak value of the CHTC is due to the correlation factor and various exponent of parameters applied in models.

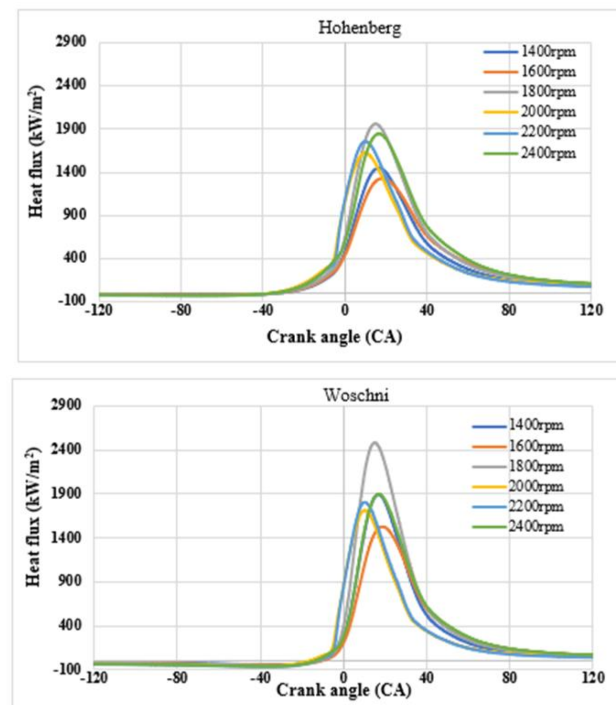

Fig. 8. Heat flux versus crank angle at low, medium, and high engine speeds for Woschni and Hohenberg models.

3.4 Heat flux

Fig. 8 shows the heat flux (Q_f) results estimated by Woschni and Hohenberg models, expressed in kW/m^2. The main parameters are fuel injection pressure (40 MPa, 90 MPa, 110 MPa) and engine speed (low, medium, and high) at full load. From Figs. 8a and b, indicate that the heat flux rises at an approximately similar CA in both Woschni and Hohenberg models at all engine speeds. From Fig. 8a the trend of peak values of heat flux is as follows: 1885 kW/m^2 (1400 rpm), 1475 kW/m^2 (1600 rpm), 2465 kW/m^2 (1800 rpm), 1670 kW/m^2 (2000 rpm), 1777 kW/m^2 (2200 rpm), and 1900 kW/m^2 (2400 rpm) from Woschni model. These peak values are higher than those obtained from the Hohenberg model by 23%, 10%, 25%, 3%, and 4%, respectively. It was discovered that the heat flux in both models was lower during the intake process because heat is added to the combustion chamber in the intake air, while the bulk gas temperature is lower than that of the cylinder wall [10], [12]. In another way, this study, similar to [21] and [23], has confirmed that the heat flux from the Woschni model overestimated in the combustion and expansion process.

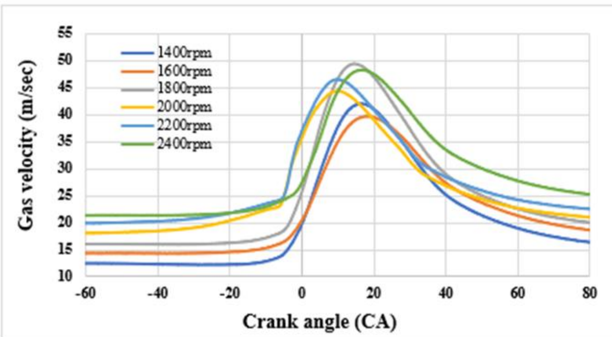

Fig. 9. Cylinder gas velocity versus crank angle at low, medium, and high engine speeds.

Furthermore, the cylinder gas velocity (*w*) in m/s against the CA at different engine speeds (low, medium, and high) and fuel injection pressure (40MPa, 90MPa, 110MPa) is shown in Fig. 9. The calculation has been done through Equation (6), as explained in section 2.4. The instantaneous cylinder gas velocity was not similar across the CA. The instantaneous cylinder gas velocity enhances as engine speeds increase, even though fuel injection pressure varies. The higher cylinder gas flow also causes the high CHTC confirmed by [30], [31].

4. CONCLUSIONS

This study used a CI engine to evaluate the heat loss from cylinder gases to the combustion chamber wall. The main parameters of the study were fuel injection pressure (40 MPa, 90 MPa, and 110 MPa) and engine speed (low, medium, and high). Two improved models, viz., Woschni and Hohenberg, were employed to estimate the instantaneous CHTC. The conclusion of the current study is summarized below:

- At moderate engine speeds and fuel injection pressure, the highest peaks of cylinder pressure were 88, 85, and 83 bar investigated at 2200, 2000, and 1800 rpm, respectively. The highest engine speed of 2400 rpm and injection pressure of 110MPa, low engine speeds (1400 rpm and 1600 rpm at 40MPa) were similar to the cylinder pressure curve.
- The cylinder temperature curves of 2000 rpm (with 90 MPa) and 2200 rpm (with 110 MPa) were seen not to follow the cylinder pressure curves.
- At all engine speeds and injection pressures, the heat release rate was sharply increased in the premixing phase and raised until its peak after the top dead center. The lowest peaks of heat release rate were investigated in the highest engine speed (2400 rpm at 110 MPa) and lowest engine speeds (1400 and 1600 rpm at 40 MPa).
- The results of CHTC from the Woschni model were higher than those of the Hohenberg model by 21.7%, 27.1% and 16.4% at 1400 rpm (40 MPa), 1800 rpm (90 MPa), and 2200 rpm (110 MPa), respectively.
- The peaks value of heat flux from the Woschni model are higher than those obtained from the Hohenberg model by 23%, 10%, 25%, 3%, and 4%, respectively.

ACKNOWLEDGEMENT

The authors would like to express their gratitude to The Joint Graduate School of energy and Environment, King Mongkut's University of Technology Thonburi, Center for Energy Technology and Environment, Ministry of Higher Education, Science, Research and Innovation Thailand for their support. Special thanks to Bangchak Corporation Public Company Limited (BCP) for supporting our tested fuel and the fuel properties test report.

REFERENCES

[1] E.C. Trujillo, F.J. Jiménez-Espadafor, J.A.B. Villanueva, M.T. García, 2011. Methodology for the estimation of cylinder inner surface temperature in an air-cooled engine. *Applied Thermal Engineering,* Elsevier, December, 31 (8-9), pp. 1474.

[2] Z. Zak, M. Emrich, M. Takats, J. Majcek, 2016, In-cylinder heat transfer modelling, *Journal of Middle European Construction and Design of Cars,* February, 14(3).

[3] L. Fonseca, R. Novella, P. Olmeda, R.M. Valle, 2019. Internal combustion engine heat transfer and wall temperature modeling: An Overview. *Archives of Computational Methods in Engineering.* 27(5):1661-1679.

[4] A. Franco, and L. Martorano, 1999, Methods to evaluate in-cylinder heat transfer and thermal load in the small internal combustion engines, December, *SAE International Journal of Engines* 108(3):1789-1803.

[5] A. Broatch, P. Olmeda, X. Margot, and J. Escalona, 2020. Conjugate heat transfer study of the impact of 'thermo-swing' coatings on internal combustion engines heat losses, *International J of Engine Research*.

[6] P. Tamilporai, N. Baluswamy, P. M. Jawahar, S. Subramaniyam, S. Chandrasekaran, K. Vijayan, S. Jaichandar, J. J. Rani, K. Arunachalam, 2003. Simulation and analysis of combustion and heat Transfer in low heat rejection diesel engine using two-zone combustion model and Ddfferent heat Transfer Models, *SAE International*, vol. 112, pp. 1185-1203.

[7] C. S. Wang, and G. F. Berry, 1985. Heat transfer in internal combustion engines, *The American Society of Mechanical Engineers*, 345 E. 47 St., New York, N.Y. 10017.

[8] J. Chang, O. Güralp, Z. Filipi, and D. Assanis, 2004. New heat transfer correlation for an HCCI engine derived from measurements of instantaneous surface heat flux, *Society of Automotive Engineers*, 2004-01-2996.

[9] K. Arato, and T. Takashima, 2015. A Study on reduction of heat Loss by optimizing combustion chamber shape, January, *SAE International Journal of Engines* 8(2):596-608.

[10] A. A. Hairuddin, P. Andrew, Wandel and Y. Talal, 2013. Effect of different heat transfer models on a diesel homogeneous charge compression ignition engine, December *IJAME* ISSN: 2229-8649, Vol. 8, 92-1304.

[11] A. Irimescu, 2012. Convective heat transfer equation for turbulent flow in tubes applied to internal combustion engines operated under motored conditions, *Applied Thermal Engineering*, vol. 50, pp. 536-545.

[12] B. Menacer, A. Soualmia, C., Belhout, M. Bouchetara, 2017. The convection heat transfer rate evaluation of a 6-cylinder in-line turbocharged direct-injection diesel engine, *MECHANIKA* ISSN 1392, 1207. 2017 Volume 23(4): 528-536.

[13] S. Mauro, R. Șener, M. Z. Gül, R. Lanzafame, M. Messina, & S. Brusca, 2018. Internal combustion engine heat release calculation using single-zone and CFD 3D numerical models *International Journal of Energy and Environmental Engineering*, 9, 215–226.

[14] F. Ma, C., Zhao, F. Zhang, Z. Zhao, Z. Zhang, Z. Xie, and H. Wang, 2015. An experimental investigation on the combustion and heat release characteristics of an opposed-piston folded-cranktrain diesel engine, *Energies* 6365-6381.

[15] R. Ebrahimi, 2011. Effect of specific heat ratio on heat release analysis in a spark-ignition engine, *Scientia Iranica*, December, Volume 18, Issue 6,1231-1236.

[16] H.S. Soyhan, H. Yasar, H. Walmsley, B. Head, G.T. Kalghatgi, 2008. Evaluation of heat transfer correlations for HCCI engine modelling. *Applied Thermal Engineering*, Elsevier, (2-3), pp.541.10.1016/j.applthermaleng.2008.03.014.hal-00498971.

[17] Y. Kobashia, Y. Wanga, G. Shibataa, H. Ogawaa, K. Naganumab, 2019. Ignition control in a gasoline compression ignition engine with ozone addition combined with a two-stage direct-injection strategy, *Fuel*, 249 (2019) 154–160.

[18] A. M. Elzahaby, M. Elkelawy, H.A.E Bastawissi, S. Malla, A. M. Moneim, 2018. Kinetic modelling and experimental study on the combustion, performance and emission characteristics of a PCCI engine fueled with ethanol-diesel blends, *Egyptian Journal of Petroleum*.

[19] R. Stone, 1999. Introduction to Internal Combustion Engines, third ed., Macmillan Press Limited, Basingstoke, Hampshire.

[20] P. Falcone, M.C.D. Gennaro, G. Fiengo, L. Glielmo, S. Santini, P. 2003. Langthaler, Torque generation model for diesel engine 42nd IEEE Conference on Decision and Control, vol. 2, Hawaii, USA, December 9-12, pp. 1771-1776.

[21] A. Sanli A. N. Ozsezen, I. Kilicaslan, M. Canakci 2008. The influence of engine speed and load on the heat transfer between gases and in-cylinder walls at fired and motored conditions of an IDI diesel engine, *Applied Thermal Engineering* 1395–1404.

[22] S.L.Mohand, L. Khaled, B.Mourad, T. Mohand, 2010, Investigation on heat transfer evaluation for a more efficient two-zone combustion model in the case of natural gas SI engines. *Applied Thermal Engineering*, Elsevier, (2-3), 319.

[23] I. Truedsson, C. Rousselle, and F. Foucher, 2017 Ozone seeding effect on the ignition event in HCCI combustion of gasoline-ethanol blends, *SAE Technical Paper* 2017-01-0727.

[24] H. Hassan 1971, Unsteady heat transfer in a motored I.C. engine cylinder, Proc Instn Mech Engrs 185 (80) (1971) 1139-1148.

[25] M. C. Drake, T. D. Fansler, and A. M. Lippert 2005. Stratified-charge combustion: modeling and imaging of a spray-guided direct-injection engine. *Proceeding of Combustion Institute*, Vol. 30, 2683-2691.

[26] J. Kashdan, J. Cherel, and B. Thirouard, 2006. A Study of Combustion Structure and implications on post-oxidation under homogeneous and stratified operation in a DISI engine, *SAE Paper* 2006-01-1262.

[27] M. Prabhahar, M. Kiani, D. Kian, K. Bhaskar, S. Sendilvelan, S. Prakash, L.R. Sassykova, 2019 Studies on pongamia oil methyl ester fueled direct injection diesel engine to increase efficiency and to reduce harmful emissions, *Advanced Biofuels Applications, Technologies and Environmental Sustainability*, 217-245.

[28] M.Y.E. Selim, M.S. Radwan, S.M.S. Elfeky, 2003. Combustion of jojoba methyl ester in an indirect injection diesel engine. *Renew Energy* 28, 1401–1420

[29] A. Sanli, C. Sayin, M. Gumus, I. Kilicaslan & M. Canakci 2009. Numerical evaluation by models of load and spark timing effects on the in-cylinder heat transfer of a SI engine, Numerical Heat Transfer, Part A: Applications: *An International Journal of Computation and Methodology*, 56:5, 444-458, doi: 10.1080/10407780903244312

[30] J. Dent, S. Suliaman, 1983 Convective and radiative heat transfer in a high swirl direct 525 injection diesel engines, *SAE technical paper* 830693–831395, https://www.jstor.org/stable/44647668

[31] H.K. Rashedul, M.A. Kalam, H.H. Masjuki, A.M. Ashraful, S. Imtenan, H. Sajjad, L.K. Wee, 2014 Numerical study on convective heat transfer of a spark-ignition engine fueled with bioethanol, *International Communications in Heat and Mass Transfer* 58 (2014) 33–39.

NOMENCLATURE

B	Cylinder bore [m]
θ	Crank angle degree [CA]
S_p	Mean piston speed [m/s]
P_{firing}	Pressure in combustion mode [kPa]
h_c	Heat transfer coefficient [W/m^2. K]
A_c	Area of the cylinder [m^2]
T_w	Temperature of cylinder wall [K]
ω	Velocity of gas [m/s]
V	Cylinder volume [m^3]
V_d	Displacement volume [m^3]
T_g	Cylinder gas temperature [K]
T_{IC},	Temperature at intake valve closed [K]
V_{IC},	Volume at intake valve closed [m^3]
P_{IC}	Pressure at intake valve closed [kPa]
P_{motor}	Pressure in motoring condition [kPa]
P	Cylinder pressure [kPa]
Q_{ht}	Instantaneous heat transfer [kW]
dU/dt	Derivative of Internal energy w.r.t time
dW/dt	Derivative of work done w.r.t time
dQht/dt	Derivative of heat loss w.r.t time
HCCI	Homogenous charge compression ignition
CFD	Computation fluid dynamics
ECU	Electronic control unit
HRR	Heat release rate
C_1 & C_2	Combustion and expansion
CA	Crank angle
C_v	Specific heat at constant volume
CHTC	Connective heat transfer coefficient